Effects of concavity on tensile and fatigue properties in fibre laser welding of automotive steels

D. Westerbaan[1], D. Parkes[2], S. S. Nayak*[1], D. L. Chen[2], E. Biro[3], F. Goodwin[4] and Y. Zhou[1]

DP980 dual phase and high strength low alloy (HSLA) steels were welded, using fibre laser, with varying amounts of concavity to determine its effects on the tensile and fatigue properties. Higher concavity, 25 to 35%, was observed to reduce the tensile strength of the DP980 welds, while not affecting the tensile strength of HSLA welds. All welds exhibited lower fatigue resistance compared to their base metals. However, DP980 welds with higher concavity (25 to 35%) exhibited even lower fatigue resistance while HSLA welds showed similar performance regardless of changes in concavity. Concavity could be minimised by reducing welding power and increasing the welding speed.

Keywords: Fibre laser welding, Dual phase steel, High strength low alloy steel, Concavity, Fatigue, Softening

Introduction

In the automotive industry the demand for laser welded blanks (LWBs), also known as tailor welded blanks, has increased over the last decades owing to the need to reduce vehicle weight and CO_2 emissions. Laser welded blanks consist of two or more sheets of similar or different materials, properties, thickness, and surface conditions which are welded together to form a blank. Laser welded blanks are generally fabricated in the butt joint configuration to form an assembly, which is subsequently formed to make the desired three-dimensional shapes.[1,2] In general, LWBs are made with conventional mild (low carbon) steel or interstitial free steel; however, in recent years the weight reduction potential of LWBs has been increased via material down gauging by employing stronger steels like high strength low alloy (HSLA) steel and advanced high strength steel (AHSS).[1,2] Implementation of HSLA and AHSS increases the material strength without compromising crashworthiness of the vehicle body structures.[2] Thus, it is important to study the weldability of automotive steels like HSLA and AHSS via laser welding.

Advanced high strength steel comprises different steel groups such as dual phase (DP) steel, transformation induced plasticity steel, complex phase steel, martensitic steel and twinning induced plasticity steel; all of which are characterised by yield strength and ultimate tensile strength (UTS) higher than 300 and 600 MPa respectively.[2,3] Among all the AHSS, DP steel is increasingly used in autobody parts because of its excellent formability for its strength and low manufacturing cost compared to other AHSS. Dual phase steel microstructure consists of a ferrite matrix embedded with martensite and/or bainite.[2,4,5] Although DP steel is increasingly used, many parts of the autobody are still made of HSLA steel, which has excellent formability and sufficient strength attributed to its microstructure consisting of a fine grained ferrite matrix with uniformly distributed ultrafine alloy carbides.[2]

DP steels have numerous advantages for use in autobody structures, but issues of weldability may arise because of high alloying additions, metastable phases within the microstructure, and the presence of zinc coating, which is common in all thin gauge automotive steels.[2] Heat affected zone (HAZ) softening is an important issue in DP steel weldments, which is still not fully understood and continues to be investigated.[6,7] Heat affected zone softening leads to a local drop in hardness below that of the base metal (BM), which may reduce the tensile strength and the fatigue life of DP steel weldments.[8–13] It has been reported that increasing welding speed reduces softening resulting in welds with tensile strength closer to that of the BM.[14] Fibre laser welding (FLW) is capable of welding at very high speed and therefore is beneficial for making LWBs.[15–18] Traditionally, laser welds have shown fatigue lives comparable to the BM;[19] however, our recent studies have indicated that fatigue life of DP steel welded by fibre laser was reduced by around 30% when compared to the BM.[8,9] Also, the stress concentration at any concavity that is present (acting like a notch) may serve as a crack initiation

[1]Department of Mechanical and Mechatronics Engineering, University of Waterloo, 200 University Avenue West, Waterloo, ON N2L 3G1, Canada
[2]Department of Mechanical and Industrial Engineering, Ryerson University, 350 Victoria Street, Toronto, ON M5B 2K3, Canada
[3]ArcelorMittal Global Research, 1390 Burlington Street East, Hamilton, ON L8N 3J5, Canada
[4]International Zinc Association, Durham, NC 27713, USA

*Corresponding author, email sashank@uwaterloo.ca

Published by Maney on behalf of the Institute
Received 18 June 2013; accepted 24 August 2013
DOI 10.1179/1362171813Y.0000000163

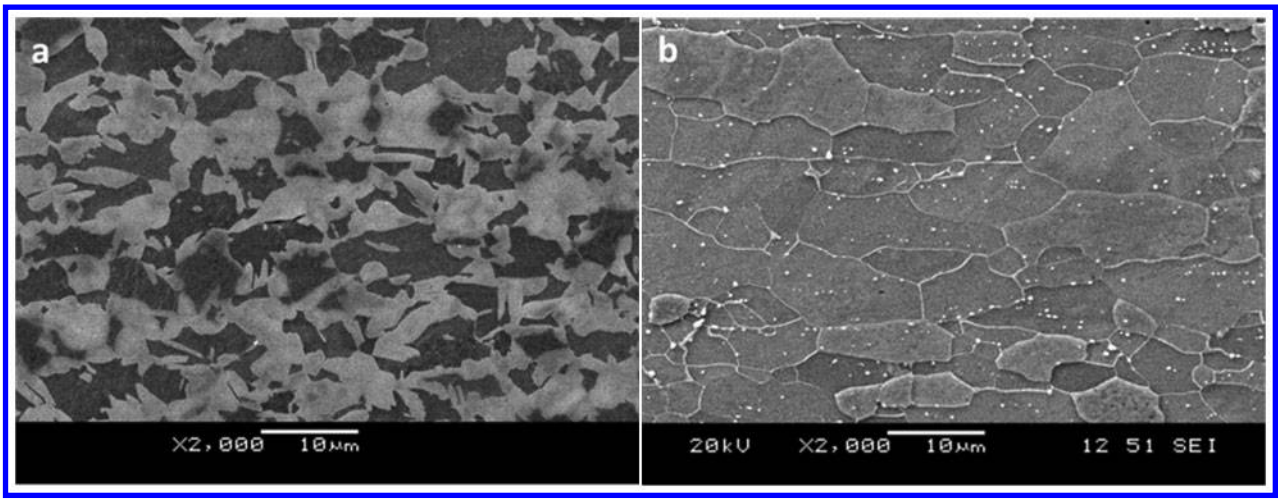

a DP980; *b* HSLA

1 BM microstructures of steels

site, which then allows cracking to propagate into the soft zone in the welds.[8] Furthermore, it should be noted that both concavity and HAZ softening have been found detrimental to the fatigue life of the DP steel welds.[8–12,20]

Concavity is formed by metal ejection or displacement from the weld pool during welding.[21] Reports have been published on simulation of the keyhole dynamics in laser welding, which indicated that metal ejection from the weld pool depends on the welding parameters.[22,23] However, metal ejection from the weld pool can also occur owing to instability of the liquid phase especially when the vapour/liquid interface within the keyhole moves normal to the laser beam at high speeds.[19] An effective way to improve the weld quality is to reduce power and speed,[24] but reduction in speed is known to increase the severity of the HAZ softening,[14] which in turn, leads to reductions in the fatigue life[12] and formability[13] of the welds. Laser welded blanks are mainly produced in butt joint configuration, which is considered one of the most difficult joints to make in laser welding because the narrow beam and high speed provide little tolerance for the beam to diverge from the seam.[24,25]

Although significant research has been reported on the microstructure and mechanical properties of AHSS and HSLA steels welded by different laser welding processes,[8–20] no study has been reported on the effects of welding parameters on the concavity and consequently on the performance of the thin gauge automotive steels like DP and HSLA. Therefore, this paper reports the effects of FLW process parameters on the concavity in DP980 (UTS $\geq$ 980 MPa) and HSLA steels. Also, the influence of the amount of concavity on the tensile and fatigue properties of the welds was investigated in order to improve the fatigue performance of fibre laser welds.

Table 1 Chemical composition (wt-%) and mechanical properties of steels used in study

Steel	DP980	HSLA
C	0·15	0·05
Mn	1·5	0·6
Si	0·3	0·1
Al	0·04	0·03
Cr	0·0	0·1
Mo	0·0	0·0
Ni	0·0	0·1
V	0·00	0·00
Fe	Bal.	Bal.
T_m/°C	1514	1527
T_{Ac1}/°C	717	721
Hardness/HV	351	145
YS/MPa	697	415
UTS/MPa	1083	461
Elongation/%	12·2	30·7

Experimental

Hot dip galvanised sheets (1·2 mm thick) of DP980 and HSLA steels were used. The chemical compositions and tensile properties of the steels are listed in Table 1 and the corresponding BM microstructures are shown in Fig. 1. DP980 steel (Fig. 1*a*) contained ferrite (dark) and martensite phase (bright) whereas HSLA steel had a ferrite matrix with uniform distribution of alloy carbides (Fig. 1*b*). The steel sheets were cut into 200 × 100 mm coupons and then joined to make a 200 × 200 mm welded blank (Fig. 2). The edges to be welded were machined flush; specimens were considered flush if they butted together with gaps less than 0·05 mm. Before welding, coupons were cleaned with acetone and were secured by clamps to ensure proper alignment. An IPG photonics YLS-6000 ytterbium fibre laser system mounted on a Panasonic TA 1600 robot was used for welding with a vertical head angle of 20° (Fig. 3), peak power of 6 kW, spot size of 0·28 mm^2, and wavelength of 1071 nm. Argon was used as shielding gas, which was blown through cross flow nozzles placed before the laser head. A large matrix of speed and power was examined to create a process envelope. All the welds were made perpendicular to the rolling direction of the sheets (Fig. 2).

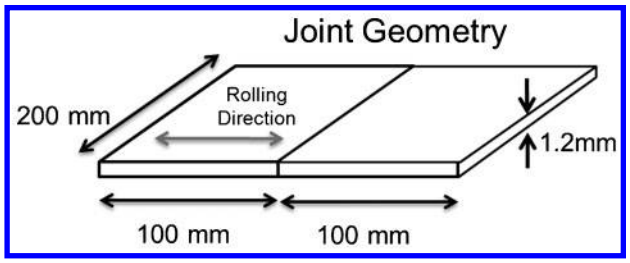

2 Schematic of joint geometry

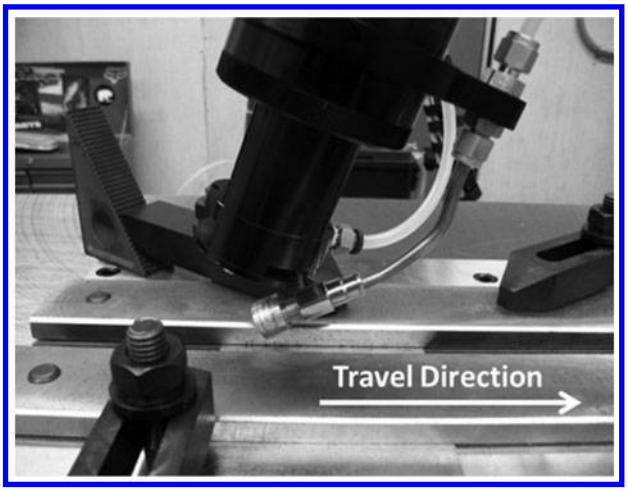

3 Head angle of laser head relative to steel sheets

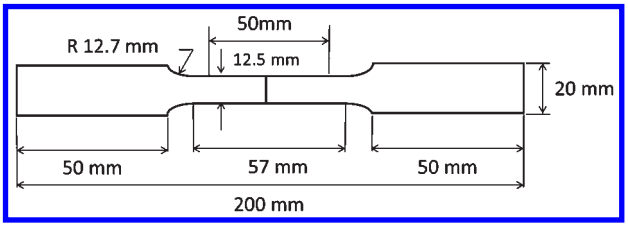

4 Schematic of tensile coupons (ASTM: E8) with weld at centre of gauge length

The weld cross-section specimens were prepared using standard metallographic procedures followed by etching with 2% nital solution. An Olympus BX51M optical microscope was used to observe the weld profiles. Concavity was measured from the weld profiles by taking the ratio of the reduction in area from the sheet thickness in the fusion zone (FZ) to the initial sheet thickness, as outlined in GM4485M.[26] For effective comparison, the measured concavity values were approximated to the nearest 5%, i.e. concavity measured as 0, 8–13, 14–16, 23–28 and 33–38% have been reported as 0, 10, 15, 25 and 35% respectively. Microhardness profiling was performed on the etched specimens in a Clemex-JS 2000 automated hardness tester under a 200 g load and 15 s dwell time. Indentations were spaced a minimum of three diameters in order to avoid interference from adjacent indents. Welds with different

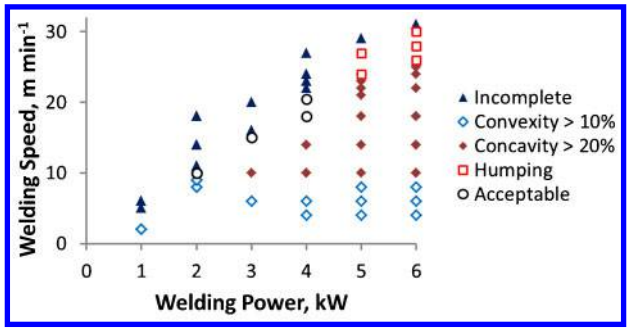

5 Process window showing welding speed–power combinations and resultant weld geometry

amounts of concavity were chosen for tensile and fatigue testing.

Transverse tensile and fatigue specimens were machined from the welds as per ASTM: E8 standards[27] with the weld positioned at the centre of the gauge length (Fig. 4). In order to remove transient effects of the laser beam, the weld start and crater were discarded before machining the specimens. Tensile tests were performed using a crosshead speed of 2·54 mm min^{-1}. For effective comparison of the welds, while minimising the error that may arise due to variation in the cross-section area along specimen gauge due to different amounts of concavity, only the peak loads obtained from the tensile tests are reported. Fatigue testing was performed according to ASTM: E466 standards[28] using a fully computerised Instron 8801 servo hydraulic testing system with a stress ratio of $R=0{\cdot}1$ applied in a sinusoidal wave at 50 Hz. A JEOL JSM 6460 scanning electron microscope was used to observe the fracture surfaces of the failed specimens. Fatigue limit was defined as the stress amplitude at which a specimen endured infinite life, i.e. sustained 1×10^7 cycles without failure.

Results and discussion

Weld concavity

The speed and power levels examined in this study are shown in Fig. 5 and example profiles of the resultant weld geometries are shown in Fig. 6. Using 6 kW full penetration welds could be made at 30 m min^{-1} (Fig. 5); however, at welding speeds higher than 22 m min^{-1} a cyclic formation of severe concavity at the top of the weld and severe convexity on the bottom of the weld occurred

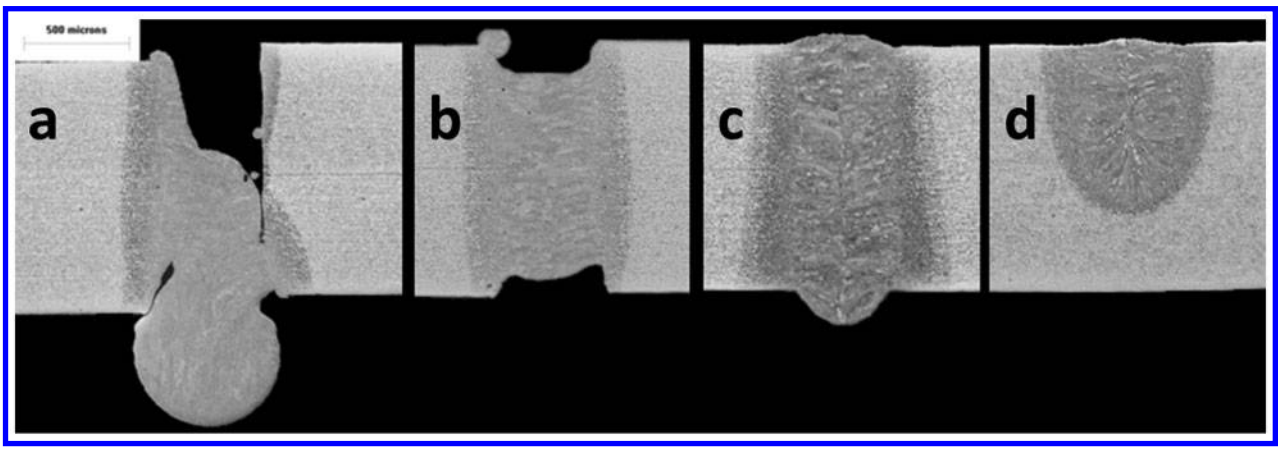

6 Typical weld profiles showing *a* humping, *b* concavity, *c* convexity and *d* incomplete penetration

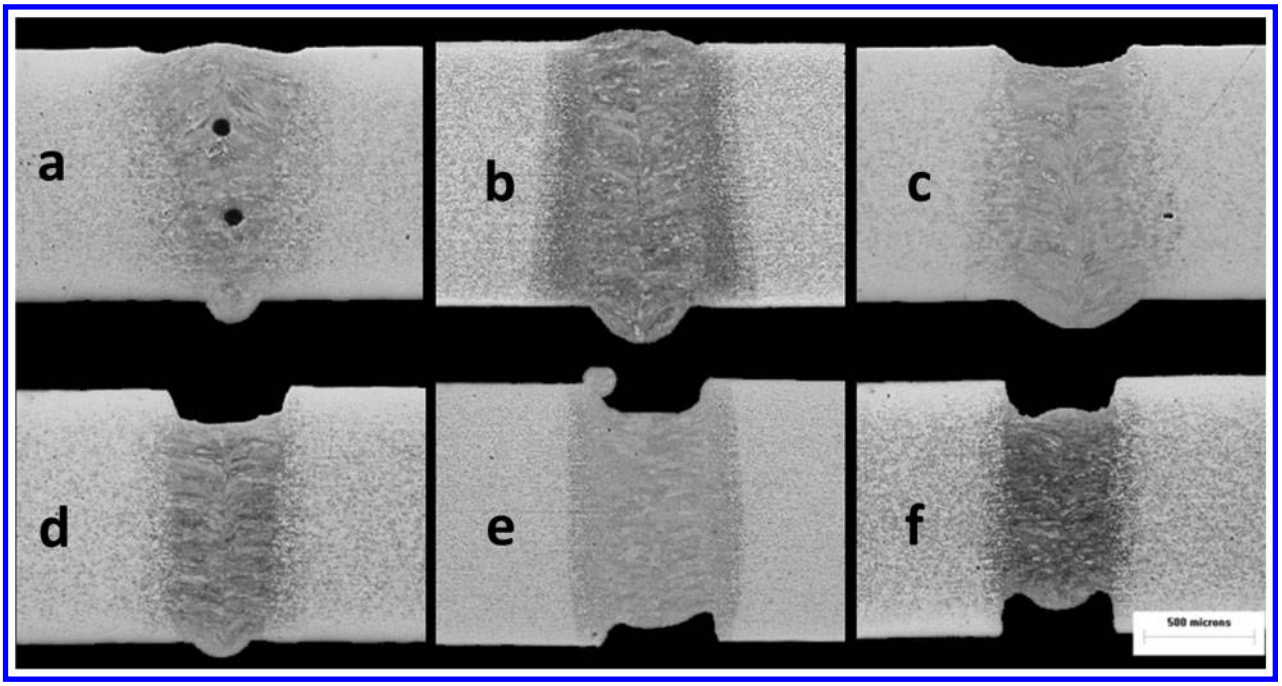

a 1 kW, 4 m min^{-1}, 0% concavity; *b* 2 kW, 10 m min^{-1}, 0% concavity; *c* 3 kW, 15 m min^{-1}, 10% concavity; *d* 4 kW, 20·5 m min^{-1}, 15% concavity; *e* 5 kW, 21 m min^{-1}, 25% concavity; *f* 6 kW, 22 m min^{-1}, 35% concavity

7 Weld profiles attained at given power level

(Fig. 6*a*), creating a discontinuous weld profile with large reduction in area from the BM; otherwise known as weld humping. Welds with humping were very weak, and could be broken by hand. Concavity occurred when weld cross-sections experienced a reduction in the area which was well wetted to the surrounding material (Fig. 6*b*). Convexity (Fig. 6*c*), being constant without cyclic formation, occurred when a continuous well wetted convex dome formed on either the top or bottom side of the weld along the length of the weldment. Incomplete penetration (Fig. 6*d*) occurred when the heat input was too low to melt through the bulk material. Welds were considered acceptable (Fig. 5) when they formed less than 20% concavity, had convexity below 10%, and were free from other defects, as per current industry standard: GM4485M.[26] Acceptable welds were made by increasing welding speed, at constant power, so that the welds just fully penetrated the sheet thickness. Accordingly, the welding speed for making acceptable welds was observed to increase with increasing power (Fig. 5). For example, using 2 kW power acceptable welds could be formed at a lower speed of 10 m min^{-1} whereas increasing the power to 4 kW required a higher speed (20·5 m min^{-1}). However, increasing power above 4 kW or decreasing it below 2 kW did not result in acceptable welds. Therefore, it was observed that to make acceptable welds in 1·2 mm thick sheets, a power range of 2–4 kW with a speed of 10–20·5 m min^{-1} was required in this study. Fully penetrating weld profiles possessing the least amount of concavity at each power level are shown in Fig. 7. Welds made at 1 kW were unacceptable because they contained porosity (Fig. 7*a*). It was also observed that the concavity increased with power (Fig. 7*b–f*).

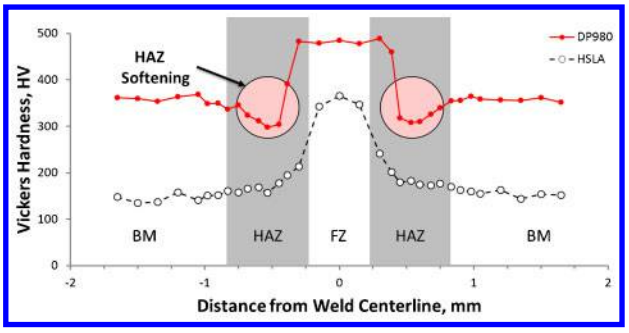

8 Typical hardness profiles of fibre laser welds of DP980 and HSLA steels made with parameters of 20·5 m min^{-1} and 4 kW

The formation of concavity owing to keyhole instability may be explained by the ejection or displacement of metal from the weld pool, which has been reported earlier.[19,21–24] However, in this study evidence of metal displacement were not observed in the weld profiles (Fig. 7) confirming that metal ejection was the only reason for concavity formation. In keyhole mode welding, evaporation of the molten metal takes place leading to an increase in vapour pressure, which pushes the vapour/liquid interface ahead of the laser beam.[19] High vapour pressure can result in higher melt velocities causing ejection of the weld metal from the front of the weld pool. Therefore, the complex liquid motion within the weld pool determines the resultant weld geometry.[19] Furthermore, a recent simulation study[22] reported that the driving force for moving the vapour/liquid interface is the vapour pressure of the keyhole. The vapour pressure depends on the available heat in the keyhole and for a constant spot size an increase in the beam power increases the vapour pressure. Thus, an increase in laser power, at any given speed, would result in a greater amount of metal ejection from the weld pool,[22] which was also observed in the present study (Fig. 7*c–f*). At any given power, welding speed controls the size of the vapour column; in other words the ability to evaporate the liquid phase and maintain a constant keyhole size is determined by the welding speed.[19]

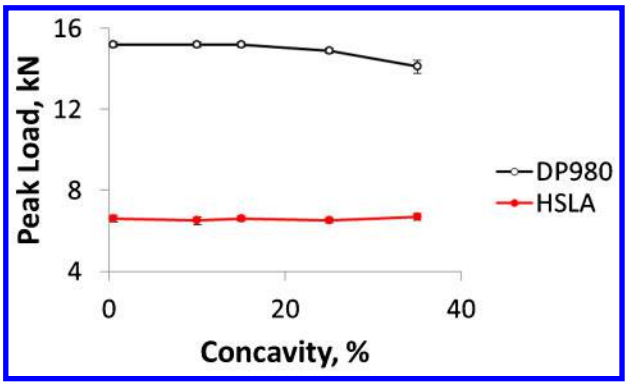

9 Peak load and concavity for welds; error bars indicate standard deviation

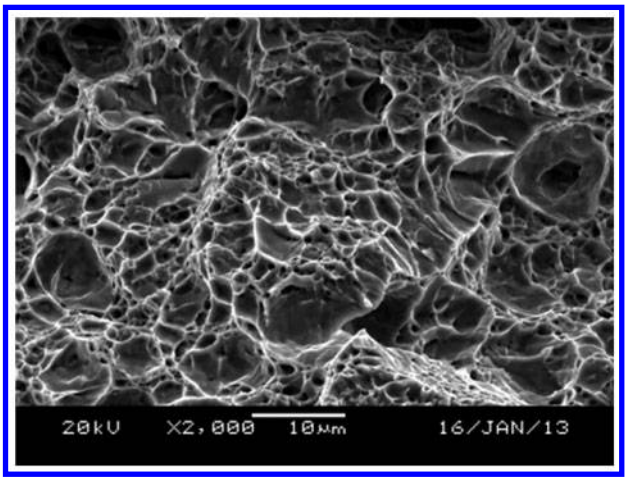

10 Ductile fracture surface of a tensile tested DP980 weld

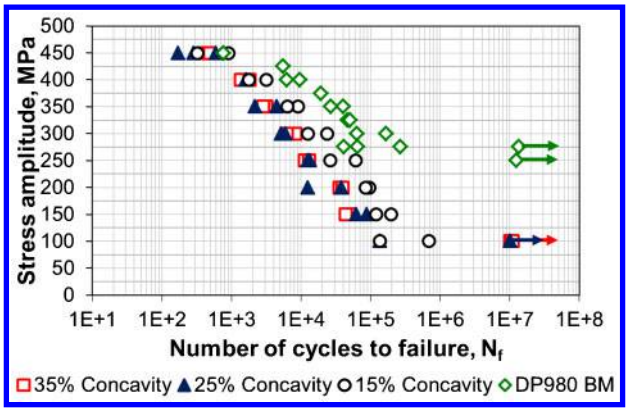

11 S–N curve of DP980 steel welds with varied amounts of concavity

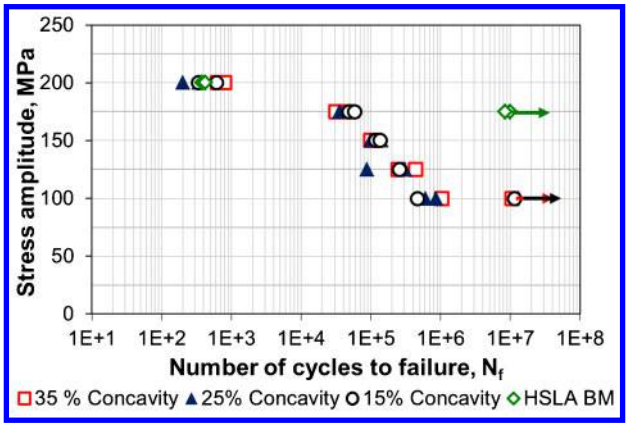

12 S–N curve for HSLA steel welds with different amounts of weld concavity

Therefore, an excessive welding speed would cause the keyhole to become unstable[19,22,24] as was observed by the erratic humping (Fig. 6*a*) formed above 22 m min^{-1} (Fig. 5). Alternatively, the welding speed determines penetration depth[21] as was observed for lower power (1–4 kW) where higher speeds yielded incomplete penetration (Fig. 5).

Microhardness and tensile properties

Figure 8 shows the hardness profiles across the welds of DP980 and HSLA steel made with 4 kW power and 20·5 m min^{-1} speed. In the FZ, DP980 steel attained higher hardness (~480 HV) than HSLA steel (~350 HV) (Fig. 8). Heat affected zone softening was detected in the DP steel, as indicated on the profile (Fig. 8) with a minimum hardness of about 300 HV; exact values are listed in Table 2. Heat affected zone softening is related to tempering of the martensite phases present in the BM (Fig. 1*a*) because the temperature experienced in this region during welding approaches the *Ac*1 temperature of the steel.[2] Heat affected zone softening was not observed in the HSLA steel because martensite was absent in its BM (Fig. 1*b*).

Tensile results (Fig. 9) indicated that increasing concavity decreased the peak load in the DP980 welds whereas HSLA welds were not affected by concavity. Data analysis performed, assuming a normally distributed sample and using *t*-tests, suggested that for DP980 there was no significant change in the peak load within 0 to 15% concavity (Table 2). Thus, welds with 15%

Table 2 Failure location and peak load of welds

Steel	Speed/m min^{-1}	Power /kW	Concavity /%	Soft zone hardness/HV	Failure location	Peak load/kN	Standard deviation	Sample size
DP980	22	6	35	306	HAZ	14·1	0·62	6
DP980	21	5	25	307	HAZ	14·9	0·26	6
DP980	20·5	4	15	302	HAZ	15·2	0·23	6
DP980	15	3	10	295	HAZ	15·2	0·24	6
DP980	10	2	0	293	HAZ	15·2	0·24	6
HSLA	22	6	35	…	BM	6·7	0·36	6
HSLA	21	5	25	…	BM	6·5	0·26	6
HSLA	20·5	4	15	…	BM	6·6	0·25	6
HSLA	15	3	10	…	BM	6·5	0·35	6
HSLA	10	2	0	…	BM	6·6	0·36	6
Hypothesis test: H_0: $x_1=x_2$ H_1: $x_1\neq x_2$					$t_{critical}$ (α=0·05/2, n_1+n_2-2)=2·776			

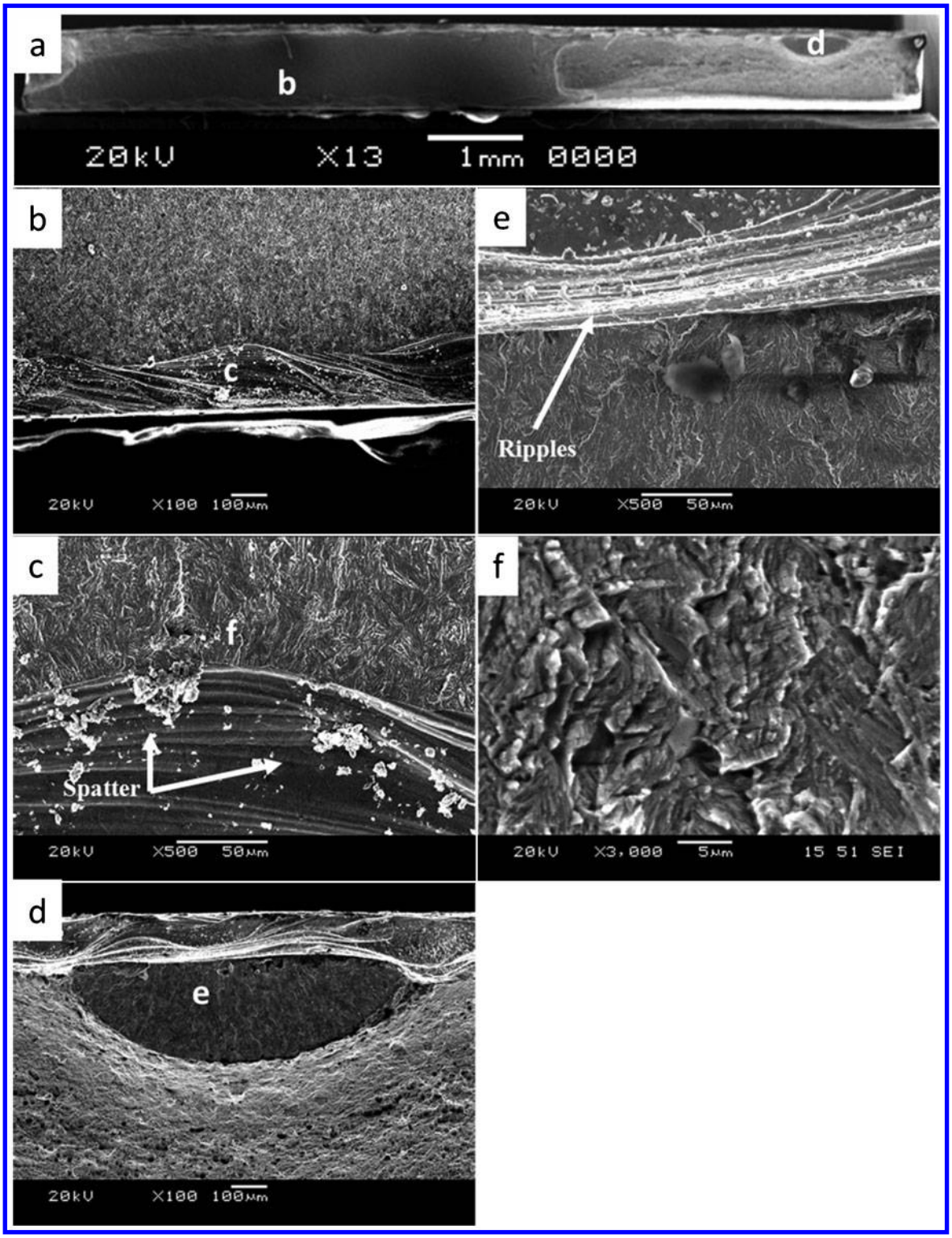

a fracture profile; *b* crack propagation leading to bottom side concavity; *c* crack initiation at weld spatter; *d* crack propagation leading to top side concavity; *e* crack intiation at ripples of weld bead; *f* brittle cleavage at initiation

13 DP980 propagation surfaces

concavity were considered acceptable with respect to tensile strength and industry standards.[26] Alternatively, when the amount of concavity increased to 25% the peak load decreased (Fig. 9) and continued to decrease with further increase in concavity (35%). A 1·1 kN drop in the peak load was observed in the DP980 steel when concavity was increased from 15 to 35% (Fig. 9 and Table 2). The DP980 welds failed in the soft zone (Table 2) where strain localisation occurred leading to premature failure,[6,13,14] which was confirmed by the fractured surface showing typical ductile dimple morphology (Fig. 10). The decrease in peak load for welds with 25 and 35% concavity was attributed to the increased amount of concavity but not to the softening since the amount of softening was reduced (Table 2); it was expected that reduced softening would increase the

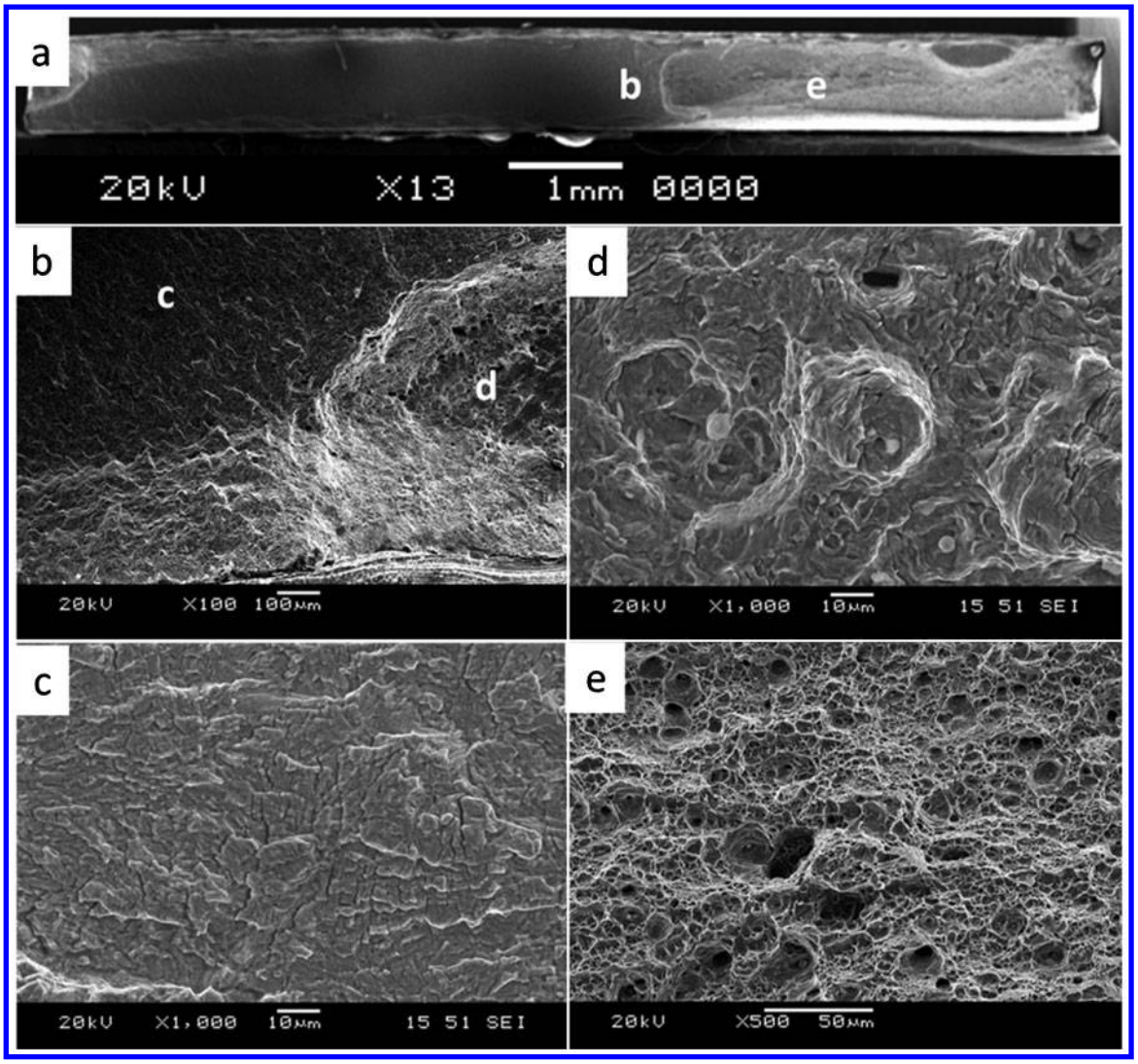

a fracture profile (same as Fig. 13*a*); *b* transition from brittle to ductile fracture; *c* brittle propagation in FZ; *d* cup–cone and brittle cleavage mix; *e* ductile cup–cone fracture surface

14 DP980 weldment final fracture surfaces

tensile strength as observed in previous studies.[6,7] Although all welds failed in the soft zone, it is believed that the higher stress concentration, caused by larger concavity (acting like a notch), reduced the peak load leading to premature failure in the soft zone.

HSLA steel always fractured in the BM (Table 2) and increasing concavity was not observed to influence the peak load (Fig. 9). The HSLA steel exhibited a resistance to the concavity because, unlike the DP980 steel, the HAZ in HSLA steel was stronger compared to the BM (Fig. 8) and therefore deformation was concentrated in the weaker BM. Thus, based on the reduced concavity, reduced softening and higher peak load, 4 kW power with a welding speed of 20·5 m min^{-1} were considered the best welding parameters, resulting in only 15% concavity (Fig. 9).

Fatigue resistance

S–N curves of the DP980 and HSLA welds are shown in Figs. 11 and 12 respectively. At a higher stress amplitude (450 MPa for the DP980 steel and 200 MPa for the HSLA steel), all welds exhibited a fatigue resistance similar to their respective BM as observed in previous studies.[8,9]

At moderate stress amplitudes (350 to 150 MPa for the DP980 steel and 175 to 100 MPa for the HSLA steel), a significant reduction in the fatigue life of all the welds was observed when compared to the BM (Figs. 11 and 12). DP980 steel welds having higher concavity (25 and 35%) demonstrated an even further reduction in fatigue resistance at moderate stress amplitudes (Fig. 11) compared to welds with lower concavity (15%); while HSLA welds with different amounts of concavity showed similar fatigue resistance. This difference in concavity (notch) sensitivity could be attributed the difference in weld hardness in both steels. The lower hardness (Fig. 8), and thus more ductile HSLA welds, would yield lower notch sensitivity than the harder DP980 welds.[29] However, the reductions in ductility and changes in the weld geometry, as will be shown later, still decreased the fatigue resistance of the HSLA welds compared to the BM (Fig. 12).

Welding reduced the fatigue limit of both the steels; DP980 welds showed a 63% reduction while HSLA steel showed a 43% reduction when compared to their respective BM. For DP980 welds, lower concavity (15%) welds did not yield infinite life unlike the higher

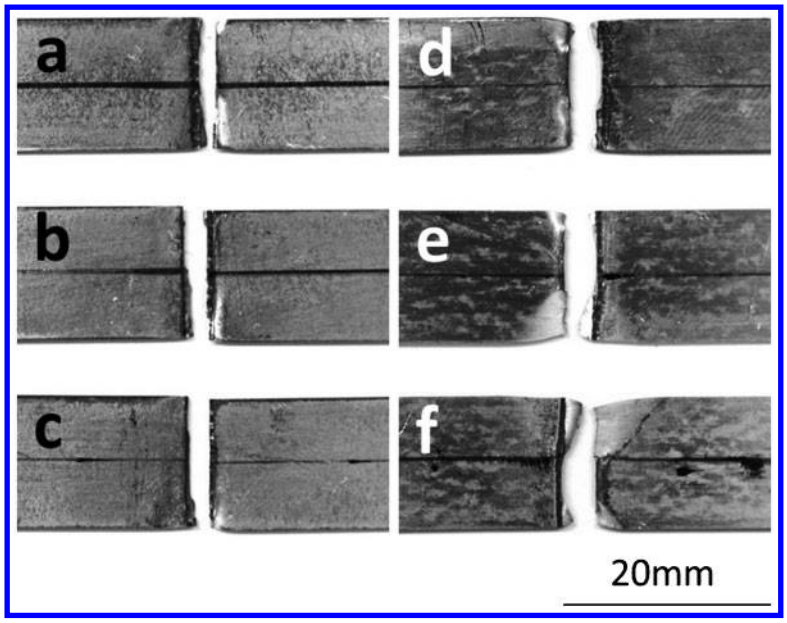

15 Macroimages of fractured low stress amplitude fatigue samples: DP980 with *a* 15%, *b* 25% and *c* 35% concavity; and HSLA with *d* 15%, *e* 25% and *f* 35% concavity

concavity (25 and 35%) welds (Fig. 11); possible reasons are discussed later in this section.

The fatigue fracture surfaces of the DP980 welds showed that the cracks initiated at the surface defects in the FZ on the concavity and then propagated throughout the FZ (Fig. 13*a*). The crack initiation was determined by the radiating structures from the concavity (Fig. 13*a*), which were seen to start either at the bottom side of the concavity (Fig. 13*b*) where weld spatters were present (Fig. 13*c*) or at the topside of the concavity (Fig. 13*d*) where ripples in the weld bead created surface discontinuities (Fig. 13*e*). The crack then propagated through the highly hardened (Fig. 8), and thus more notch sensitive, FZ as confirmed by the cleavage morphology (Fig. 13*f*). Fig. 14*a* and *b* shows a transition from brittle cleavage like fracture (Fig. 14*c*) to a mixture of brittle cleavage and ductile dimple morphology (Fig. 14*d*). The final fracture surface demonstrated a typical dimple structure (Fig. 14*e*), which confirmed that final fracture in the DP980 welds occurred in the soft zone. Fracture propagation into the soft zone was also observed by the slight necking (bright regions), at the outer edges of the fractured specimens (Fig. 15*a*–*c*).

For HSLA steel welds, fatigue crack initiation began at surface discontinuities owing to ripples formed in the areas of high concavity (Fig. 16*a* and *b*), which then propagated through the harder FZ until stress was concentrated at the edges of the specimen. In the failed specimens necking was observed (Fig. 15*d*–*f*), which resulted in ductile failure as indicated by typical dimple morphology (Fig. 16*c*). For HSLA welds, the observed deformation was more uniform indicating that the final

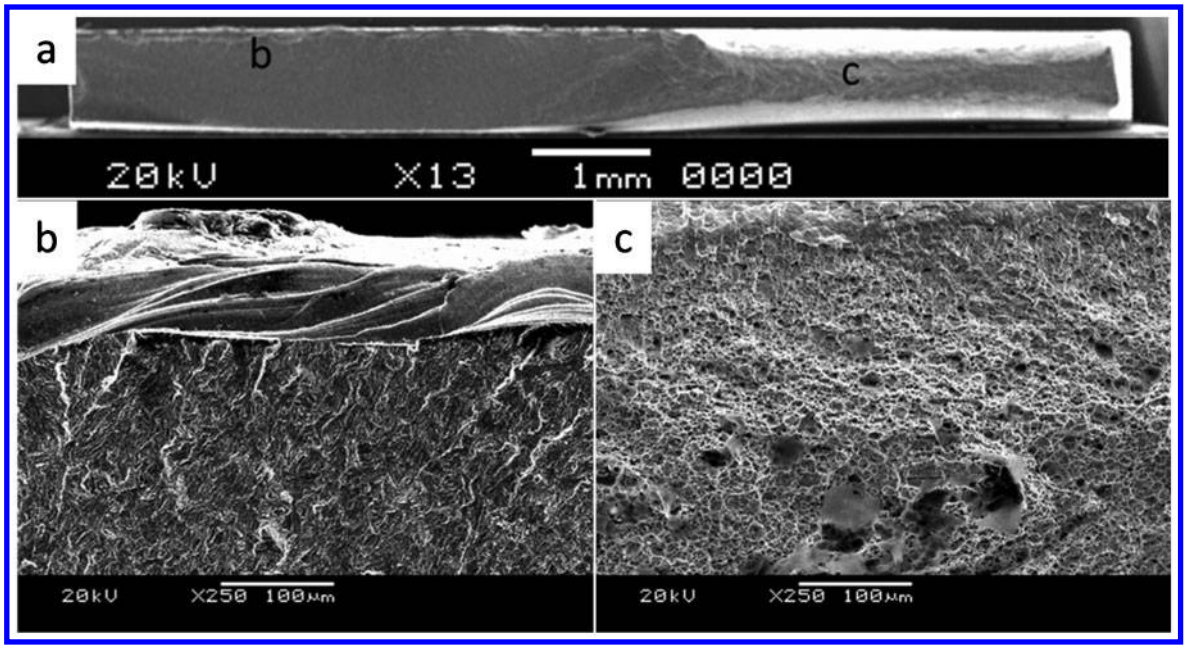

a fracture surface; *b* crack initiation at ripples of weld bead; *c* cup–cone fracture pattern of final fracture

16 HSLA fracture profile

fracture occurred in the BM, as confirmed by the large amount of necking at the outer edges of the failed specimens (Fig. 15*d–f*), with fracture propagating through the harder FZ and HAZ.

Surface discontinuities in the DP980 welds were observed to have a significant effect on the fatigue life at the low stress amplitudes (Fig. 11), which is well supported by literature.[29] It should be recalled that the welds with 15% concavity were made at a speed so that the laser just fully penetrated the sheet thickness (Fig. 7*d*), which formed weld spatters on the bottom side of the weld (Fig. 13*c*). The weld spatters acted as crack initiation sites and reduced the fatigue life of the DP980 welds with 15% concavity, compared to the welds with higher amounts of concavity which attained infinite life (Fig. 11). The ease of crack initiation at the spatters, compared to the ripples on the weld bead, decreased the fatigue life of welds with spatter at low stress amplitude. Thus, it was concluded that concavity had a significant effect on the fatigue resistance of DP980 steel welds at moderate stress amplitudes (350–150 MPa), while the surface conditions dominated the fatigue life at lower stress amplitude.

Conclusions

Weld geometry, microhardness, tensile and fatigue properties of DP980 and HSLA steel sheets welded by FLW were studied with a special focus on the effects of concavity and consequently on the performance of the welds. The following conclusions were drawn from this study.

1. By reducing power and increasing speed, weld concavity of DP980 and HSLA steels could be reduced.

2. Higher concavity, 25 to 35%, was observed to reduce the tensile strength of the DP980 welds, while not affecting the HSLA welds.

3. At high stress amplitudes (450 MPa for DP980 and 200 MPa for HSLA) all the welds showed similar fatigue resistance as their respective BM. However, both DP980 and HSLA welds demonstrated lower fatigue resistance than their BM at lower stress amplitudes.

4. For DP980 welds, higher amounts of concavity (25 and 35%) further reduced the fatigue resistance at moderate stress amplitudes (350 to 150 MPa). In contrast, HSLA welds exhibited similar fatigue resistance despite the variation in concavity; attributed to the lower FZ hardness and hence lower concavity (notch) sensitivity of HSLA.

Acknowledgements

This research was funded by the International Zinc Association, USA; AUTO21, Canada's automotive research and development program, Initiative for Automotive Manufacturing Innovation (IAMI). The authors are thankful to Dr Scott Lawson for the valuable discussion. The help of ArcelorMittal Dofasco Inc. in Hamilton, Canada in providing materials for this study is highly acknowledged.

References

1. Auto/Steel Partnership: 'Advanced high strength steel applications, design and stamping process guidelines', Southfield, MI, Jan 2010, e-book available at: http://www.a-sp.org
2. World Auto Steel: 'Advanced high strength steel (AHSS) application guidelines', Version 4·1, 1–30; June 2009, e-book available at: www.worldautosteel.org
3. F. C. Campbell (ed.): 'Elements of metallurgy and engineering alloys', 387–391; 2008, Materials Park, OH, ASM International.
4. H. K. D. H. Bhadeshia and R. W. K. Honeycombe: 'Steels: microstructure and properties', 3rd edn, 220–223; 2006, Cambridge, Oxford, Elsevier.
5. R. G. Davies: 'The deformation behaviour of a vanadium-strengthened dual phase steel', *Metall. Trans. A*, 1978, **9A**, 41–52.
6. M. Xia, E. Biro, Z. Tian and Y. Zhou: 'Effects of heat input and martensite on HAZ softening in laser welding of dual phase steels', *ISIJ Int.*, 2008, **48**, (6), 809–814.
7. E. Biro, J. McDermid, J. Embury and Y. Zhou: 'Softening kinectics in the subcritical heat-affected zone of dual-phase steel welds', *Miner., Met. Mater. Soc. A*, 2010, **41A**, 2348–2356.
8. W. Xu, D. Westerbaan, S. S. Nayak, D. L. Chen, F. Goodwin, E. Biro and Y. Zhou: 'Microstructure and fatige performance of single and multiple linear fiber laser welded DP980 dual-phase steel', *Mater. Sci. Eng. A*, 2012, **A553**, 51–58.
9. W. Xu, D. Westerbaan, S. S. Nayak, D. L. Chen, F. Goodwin and Y. Zhou: 'Tensile and fatigue properties of fiber laser welded high strength low alloy', *Mater. Des.*, 2012, **43**, 373–383.
10. N. Farabi, D. L. Chen and Y. Zhou: 'Microstructure and mechanical properties of laser welded dissimilar DP600/DP980 dual-phase steel joints', *J. Alloys Compd*, 2011, **509**, 982–989.
11. N. Farabi, D. L. Chen, J. Li, Y. Zhou and S. Dong: 'Microstructure and mechanical properties of laser welded DP600 steel joints', *Mater. Sci. Eng. A*, 2010, **A527**, 1215–1222.
12. D. Anand, D. L. Chen, S. D. Bhole, P. Andreychuck and G. Boudreau: 'Fatigue behaviour of tailor (laser)-welded blanks for automotive applications', *Mater. Sci. Eng. A*, 2006, **A420**, 199–207.
13. S. K. Panda, N. Sreenivasan, M. Kuntz and Y. Zhou: 'Numerical simulations and experimental results of tensile test behavior of laser butt welded DP980 steels', *J. Eng. Mater. Technol.*, 2008, **130**, 041003-1-9.
14. N. Sreenivisan, M. Xia, S. Lawson and Y. Zhou: 'Effect of laser welding on formability of DP980 steel', *J. Eng. Mater. Technol.*, 2008, **130**, 041004-1-9.
15. D. Westerbaan, S. S. Nayak, D. Parkes, W. Xu, D. L. Chen, S. D. Bhole, F. Goodwin, E. Biro and N. Zhou: 'Microstructure and mechanical properties of fiber laser welded DP980 and HSLA steels', Proc. SMWC XV, Detriot, MI, USA, October 2012, AWS, 3/1–13.
16. J. Canning: 'Fiber lasers and related technologies', *Opt. Lasers Eng.*, 2005, **44**, 645–676.
17. E. Assuncao, L. Quintino and R. Miranda: 'Comparative study of laser welding in tailor blanks for the automotive industry', *Int. J. Adv. Manuf. Technol.*, 2012, **49**, 123–131.
18. B. Rooks: 'Tailor-welded blanks bring multiple benefits to car design', *Assem. Autom.*, 2001, **21**, (4), 323–328.
19. W. W. Duley: 'Laser welding', 94–113; 1999, New York, John Wiley & Sons, Inc.
20. R. S. Sharma and P. Molian: 'Yb:YAG laser welding of TRIP780 steel with dual phase and mild steels for use in tailor welded blanks', *Mater. Des.*, 2009, **30**, 4146–4155.
21. Y. Kawahito, M. Mizutani and S. Ktayama: 'Elucidation of high-power fibre laser welding phenomena of stainless steel and effect of factors on weld geometry', *J. Phys. D: Appl. Phys.*, 2007, **40**, 5854–5859.
22. C. Chan and J. Mazumder: 'One-dimensional steady-state model for damage by vaporization and liquid expulsion due to laser-material interaction', *J. Appl. Phys.*, 1987, **62**, (11), 4579–4586.
23. J. Mazumder: 'Overview of melt dynamics in laser processing', *Opt. Eng.*, 1991, **30**, (8), 1208–1219.
24. C. Dawes: 'Laser welding', 117–132; 1992, New York, McGraw-Hill, Inc.
25. M. Ono, A. Yoshitake and M. Omura: 'Laser wedlability of high-strength steel sheets in fabrication of tailor welded blanks', *Weld. Int.*, 2004, **18**, (10), 777–784.
26. General Motors Co.: 'Weld specifications for laser welds – butt joints', GM4485M, General Motors Co., Detriot, MI, USA, 2002.
27. 'Standard test methods for tension testing of metallic materials', E8/E8M-11, ASTM International, West Conshohocken, PA, USA, 2012.
28. 'Standard practice for conducting force controlled constant amplitude axial fatigue tests of metallic materials', E466-07, ASTM International, West Conshohocken, PA, USA, 2012.
29. S. R. Lampman: 'Fatigue and fracture', Vol. 19, in 'ASM handbook', 241–320; 1996, Materials Park, OH, ASM International.